iScience, Volume *24*

Supplemental information

Atomically confined calcium in nitrogen-doped graphene as an efficient heterogeneous catalyst for hydrogen evolution

Jie Sun, Suchun Li, Qi Zhao, Cunping Huang, Qiang Wu, Wei Chen, Qunjie Xu, and Weifeng Yao

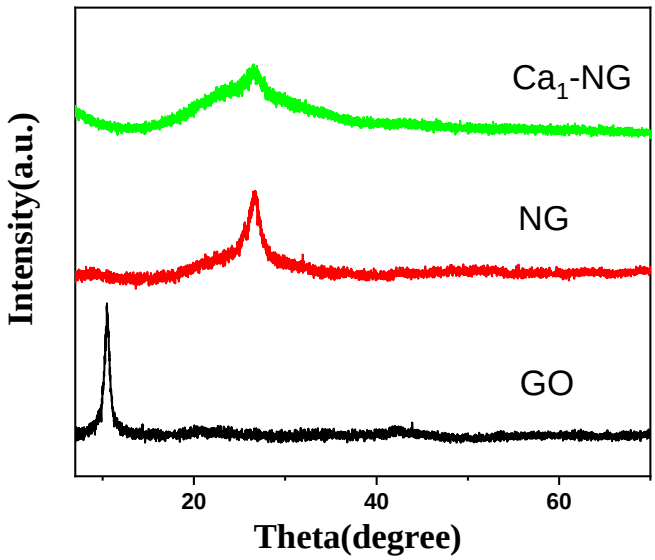

Figure S1. Related to Figure 1. XRD patterns of GO, NG and Ca_1-NG.

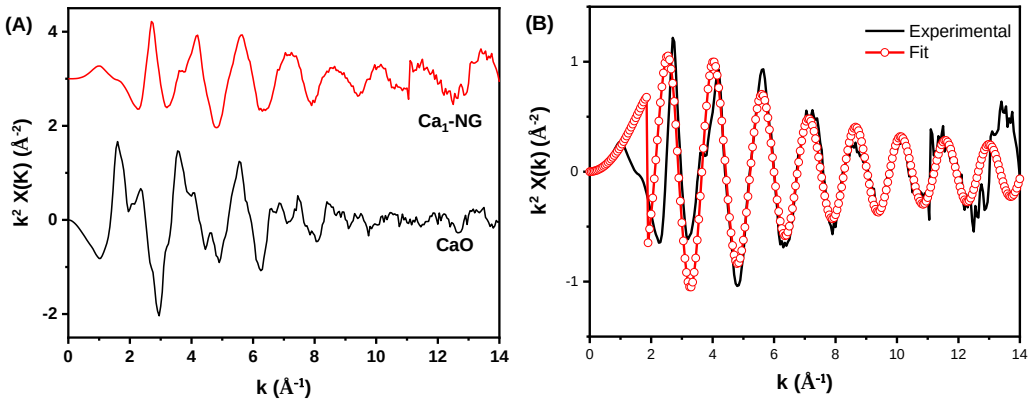

Figure S2. Related to Figure 3. Ca K-edge FT-EXAFS spectra of Ca_1-NG and the reference samples at k-space (A) and the corresponding Ca K-edge EXAFS k-space fitting curves for Ca_1-NG (B).

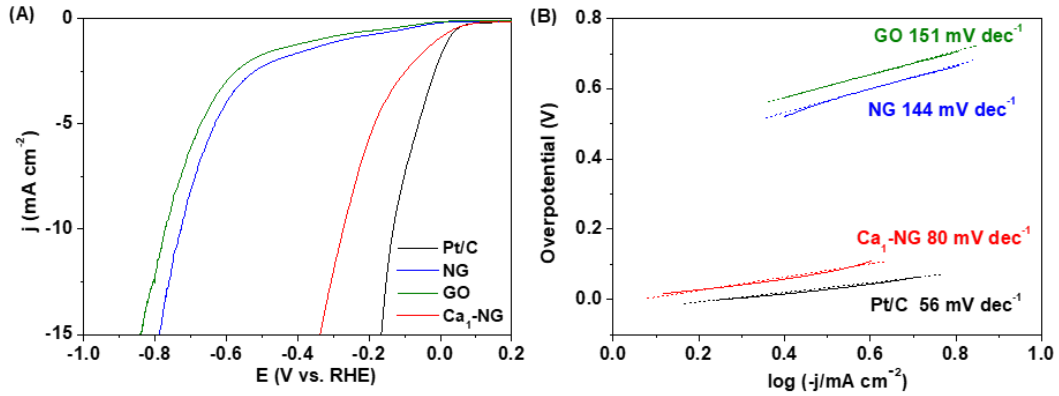

Figure S3. Related to Figure 4. (a) Polarization curves and (b) Tafel plots for HER from a 1.0 M $(NH_4)_2SO_3$ solution (pH = 8.0) on the modified GCEs comprised of GO, NG, Ca_1-NG and commercial Pt/C electrocatalysts with 0.38 mg cm^{-2} catalyst loading density.

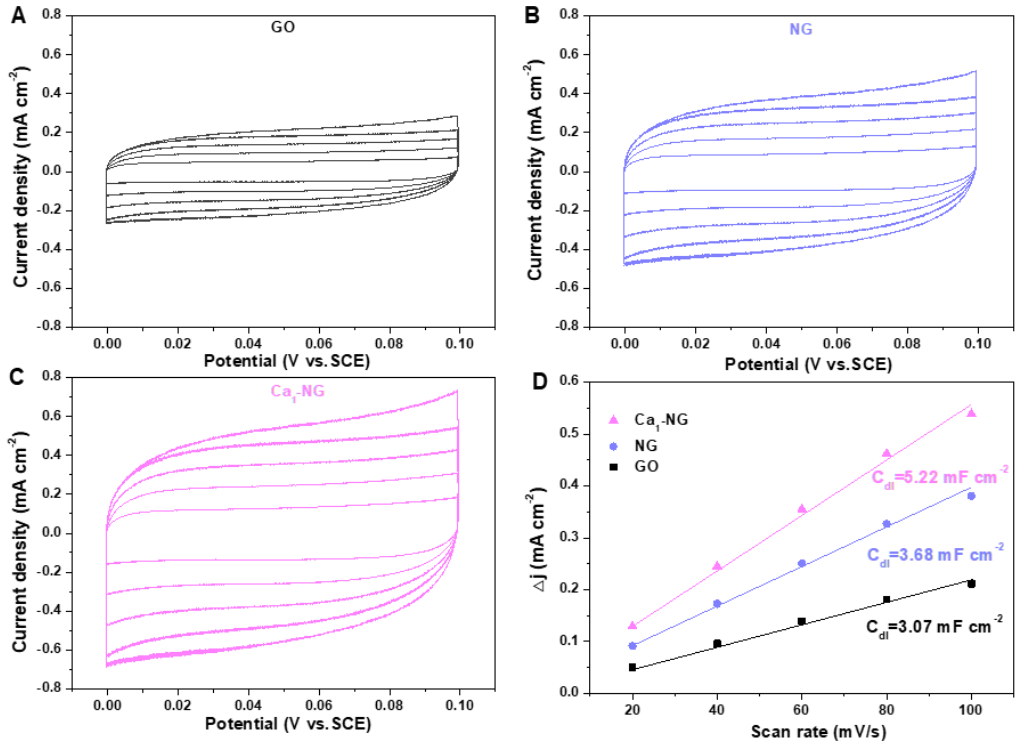

Figure S4. Related to Figure 4. Cyclic voltammograms of GO (A), NG (B), and Ca_1-NG (C) in a 0.5 M H_2SO_4 solution. The scanning rates are from 20 to 100 mV s^{-1} and the potential ranges are from 0.00 - 0.10 V vs RHE. (D) The double-layer capacitances (C_{dl}) are calculated by plotting the current density against scan rate to fit a linear regression. $\triangle j = (j_a - j_c)/2$ is obtained at 50 mV vs. RHE.

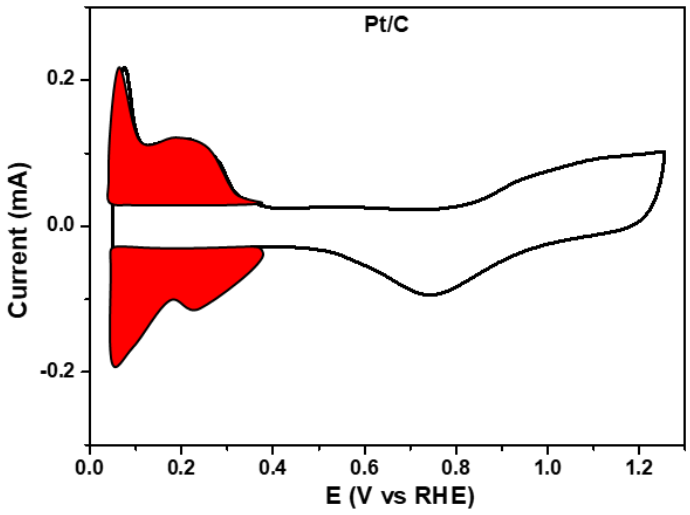

Figure S5. Related to Figure 4. Hydrogen adsorption/desorption for measuring the surface area of a 20 wt.% commercial Pt/C catalyst at 20 mV s^{-1} in Ar-saturated 0.5 M H_2SO_4.

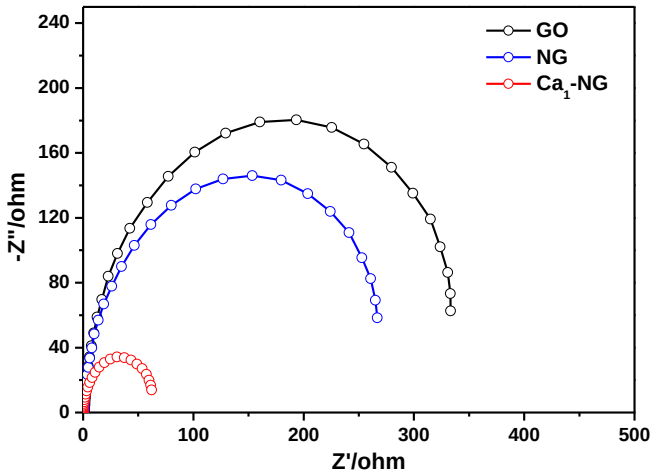

Figure S6. Related to Figure 4. Nyquist plots of GO, NG, Ca_1-NG modified graphite carbon electrodes in a 0.5 M H_2SO_4 solution.

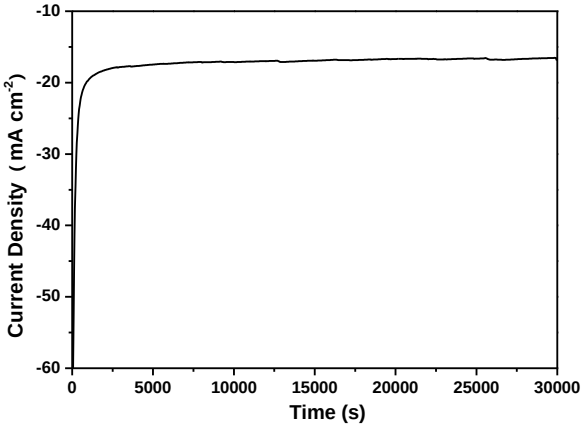

Figure S7. Related to Figure 4. Durability i-t curve of Ca_1-NG at a 200 mV (vs. RHE) constant overpotential.

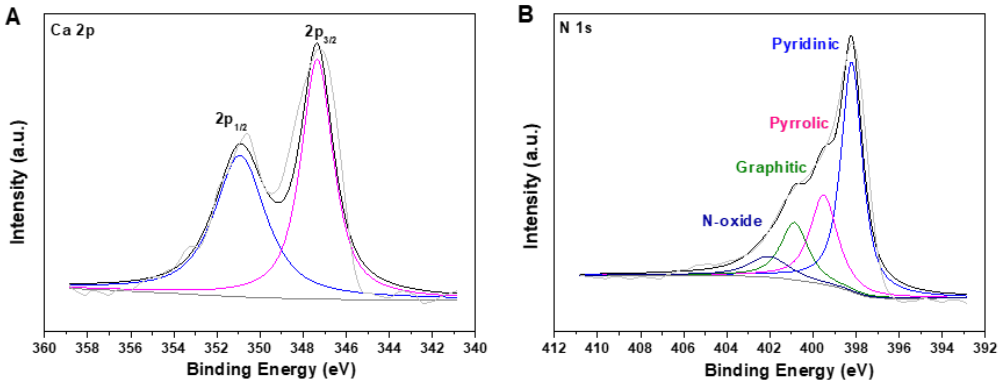

Figure S8. Related to Figure 2. (A) Ca 2p and (B) N 1s high-resolution XPS spectra of Ca_1-NG after the hydrogen evolution reaction.

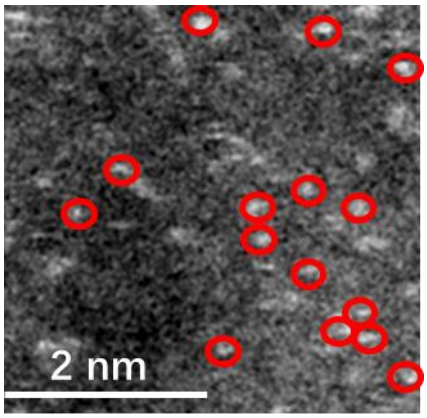

Figure S9. Related to Figure 1. HAADF-STEM image of Ca_1-NG after the hydrogen evolution reaction.

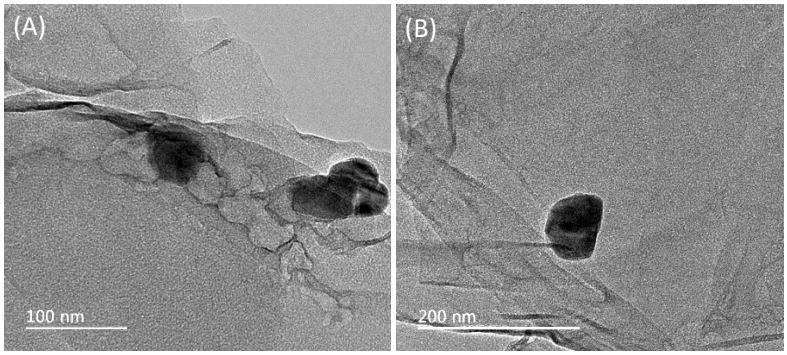

Figure S10. Related to Figure 1. TEM images of Ca_1-NG/CdS before (A) and after (B) the photocatalytic hydrogen reactions.

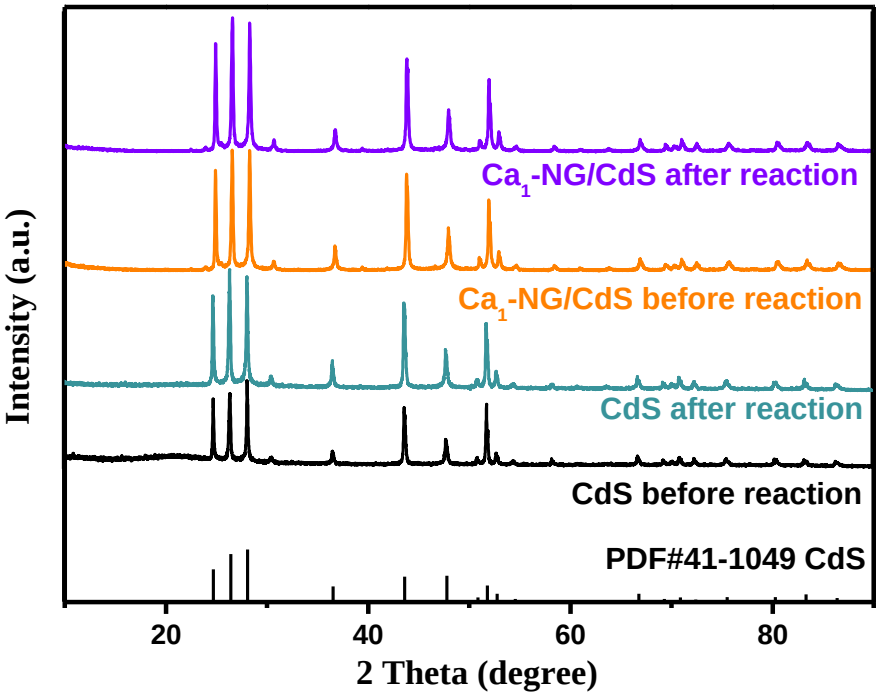

Figure S11. Related to Figure 1. XRD patterns of CdS and 0.5 wt.% Ca_1-NG/CdS before and after the photocatalytic hydrogen evolution reaction.

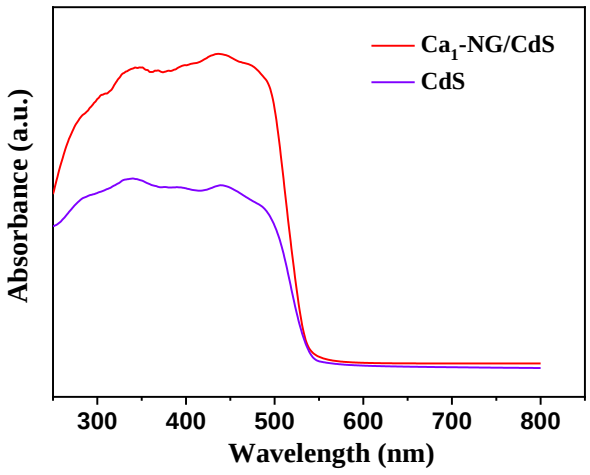

Figure S12. Related to Figure 5. UV-visible absorption spectra of CdS and 0.5 wt.% Ca_1-NG/CdS.

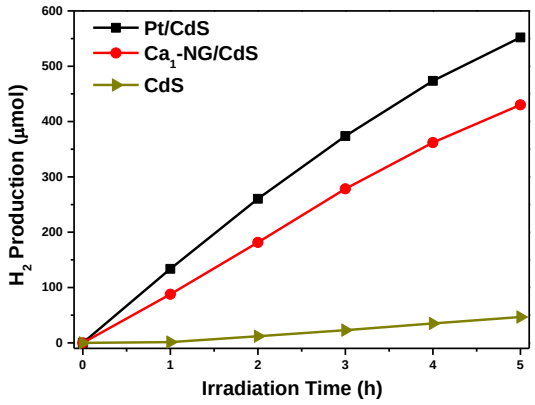

Figure S13. Related to Figure 4. Photocatalytic H_2 evolution of pure CdS, 0.5 wt.% Ca_1-NG/CdS and 0.5 wt.% Pt/CdS photocatalysts.

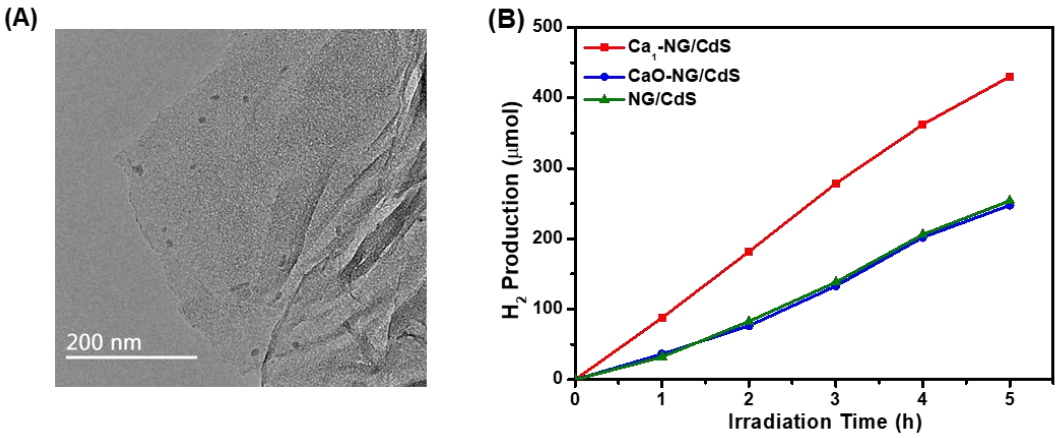

Figure S14. Related to Figure 4. (A) TEM images of CaO-NG; (B) Photocatalytic H_2 evolution of 0.5 wt.% NG/CdS, 0.5 wt.% CaO-NG/CdS and 0.5 wt.% Ca_1-NG/CdS.

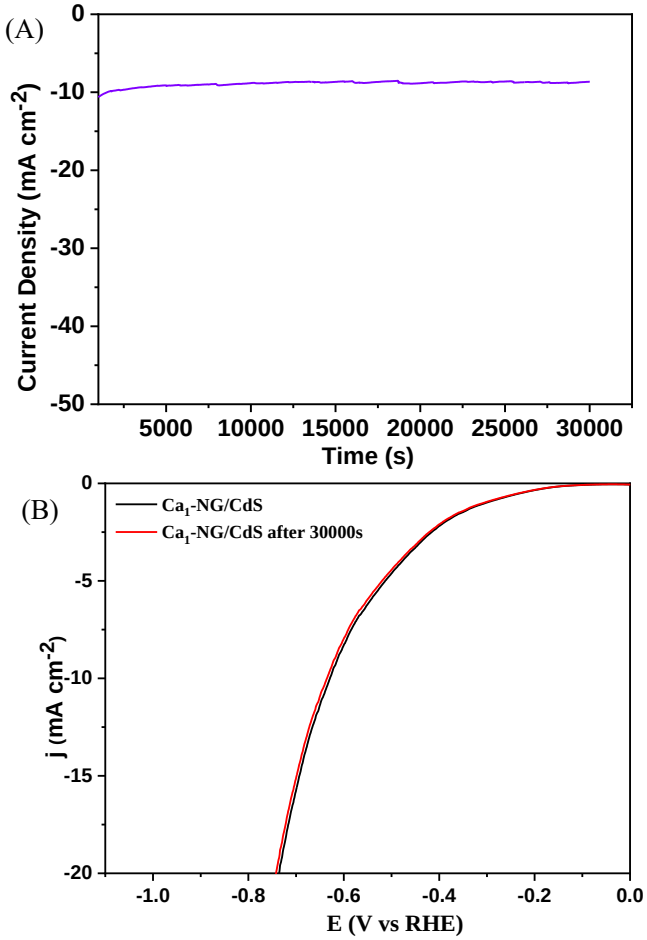

Figure S15. Related to Figure 4. (A) Time dependence of current density at -0.6 V (vs. RHE) and (B) the polarization curves of Ca_1-NG/CdS measured in 0.5 M H_2SO_4 solution before and after a 30,000 seconds stability test.

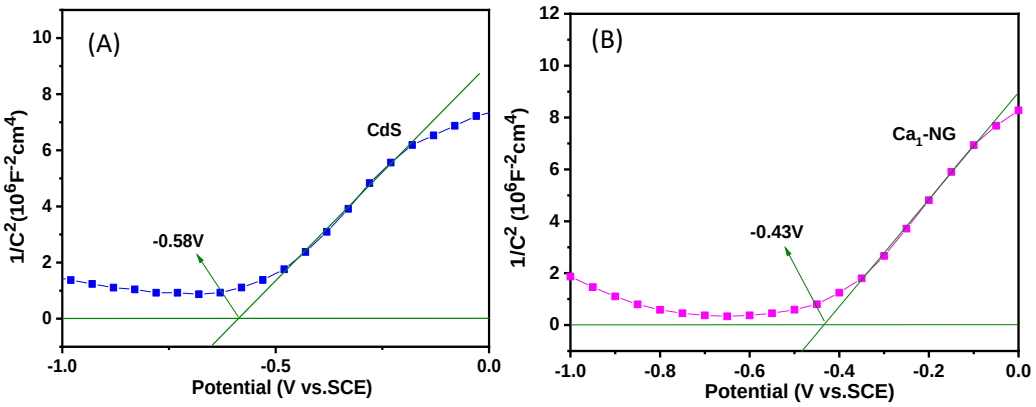

Figure S16. Related to Figure 5. Mott−Schottky plots of CdS and Ca_1-NG can be estimated as -0.58 V and -0.43 V vs. SCE, respectively.

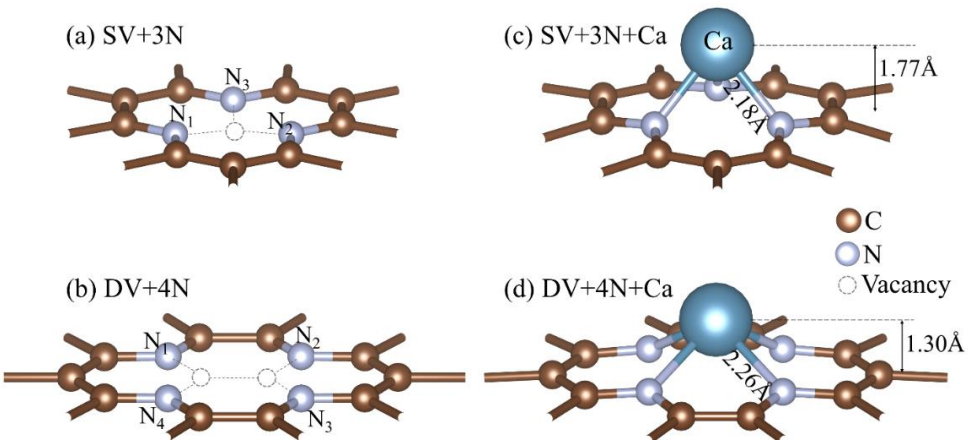

Figure S17. Related to Figure 6. Atomic structures of graphene with (a) a single vacancy + 3 pyridinic-N (SV+3N), or (b) a double vacancy + 4 pyridinic-N (DV+4N), or (c) a SV+3N plus Ca, or (d) a DV+4N plus Ca. The N atoms are symmetric around a central axis. The Ca atom is on the central axis and around 1.3~1.8 Å above the 2D plane, forming three/four identical N-Ca bonds.

Table S1. XPS data fitting results for Ca_1-NG cocatalyst. **Related to Figure 2.**

Element	Peaks	Binding Energy (eV)	FWHM (eV)	Area
N	Pyridinic N	398.0	1.7	12236.9
	Pyrrolic N	399.5	1.6	6023.4
	Graphitic N	400.8	1.8	5369.4
	Oxidized N	402.1	1.8	1368.7
Ca	Ca $2p_{3/2}$	347.2	2.4	5548.3
	Ca $2p_{1/2}$	350.8	2.3	3358.6

Table S2. EXAFS data fitting results for Ca_1-NG cocatalyst. **Related to Figure 3.**

Shell	N	ΔE (eV)	100 x R (Å)	10^3 x σ^2 ($Å^2$)	R-factor
Ca-N	2.82 (0.64)	13.59 (2.43)	241.4 (2.30)	0.13 (2.69)	0.035

Table S3. Summary of hydrogen evolution rates and quantum efficiencies for non-noble-metal based cocatalysts. **Related to Figure 4.**

Non-Noble-Metal Cocatalyst/Photocatalyst	Light Source	Sacrificial Reagent	H_2 Production Rate	Quantum Efficiency	Ref.
$ZnIn_2S_4$/CdS	300 W xenon lamp (320 nm - 780 nm)	0.25 M Na_2S and 0.35 M Na_2SO_3	3072 μmol g^{-1} h^{-1}	15.9 % at 420 nm	(Zhu, et al., 2020)
$ZnIn_2S_4$-MoS_2/CdS	300 W xenon lamp (> 420 nm)	10 vol.% TEOA	7570.4μmol g^{-1} h^{-1}	30.4 % at 420 nm	(Wang, et al., 2020)
Mo_2C/CdS	xenon lamp (> 420 nm)	20 vol.% LA	7.7 mmol g^{-1} h^{-1}	86 % at 460 nm	(Ruan, et al., 2020)
SnS_2/CdS	150 W xenon lamp with an AM 1.5G filter	20 vol.% LA	20.2 mmol g^{-1} h^{-1}	N/A	(Rangappa, et al., 2020)
Ni NPs/Ni doped CdS	300 W xenon lamp (> 400 nm)	Lactic acid	20.6 mmol g^{-1} h^{-1}	37.5 % at 420 nm	(Zhang, et al., 2020)
FeP/ CdS	300 W xenon lamp (> 420 nm)	10 vol% lactic acid	11.12 mmol g^{-1} h^{-1}	18.6 % at 450 nm	(Sun, et al., 2020)
$NiCo_2S_4$/CdS	300 W xenon lamp (> 400 nm)	Lactic acid	20.0 mmol g^{-1} h^{-1}	N/A	(Li, et al., 2019)
CoPe@GO/CdS	LED lamp (< 450 nm)	0.35 M Na_2S and 0.25 M Na_2SO_3	29.4 mmol g^{-1} h^{-1}	N/A	(Hu, et al., 2019)
NiSe/CdS	300 W xenon lamp (> 420 nm)	0.75 M Na_2S and 1.05 M Na_2SO_3	170 mmol g^{-1} h^{-1}	12 % at 420 nm	(Irfan, et al., 2019)
ReS_2/CdS	300 W xenon lamp (> 420 nm)	10 vol% lactic acid	137.5 mmol g^{-1} h^{-1}	53.6 % at 420 nm	(Ye, et al., 2019)
		Na_2S and Na_2SO_3	24.36 mmol g^{-1} h^{-1}	6.02 % at 420 nm	
CdS/g-C_3N_4	300 W xenon lamp (> 420 nm)	10 vol% lactic acid	2537 μmol g^{-1} h^{-1}	3.41 % at 420 nm	(Chen, et al., 2019)
P-MoS_2/CdS	300 W xenon	0.35 M	5.89 mmol g^{-1} h^{-}	19.0 % at 420	(Xu, et al., 2019)

	lamp (> 420 nm)	Na_2S and 0.25 M Na_2SO_3	[1]	nm	
Co_2P/CdS	300 W metal halide lamp (420 nm - 780 nm)	10 vol% lactic acid	66.98 mmol g^{-1} h^{-1}	2.26 % at 700 nm	(Li, et al., 2019)
$H_{0.53}WO_3$/CdS	300 W xenon lamp (> 420 nm)	10 vol% lactic acid	2.94 mmol g^{-1} h^{-1}	N/A	(Zhang, et al., 2019)
UiO-66@CdS/WP	300 W xenon lamp (> 420 nm)	10 vol% lactic acid	5267 μmol g^{-1} h^{-1}	N/A	(Zhang, et al., 2019)
Ti_3C_2/CdS	300 W xenon lamp (> 420 nm)	18 vol% lactic acid	14342 mmol g^{-1} h^{-1}	40.5 % at 425 nm	(Ran, et al., 2017)
WS_2/CdS	150 W xenon lamp (> 420nm)	Lactic acid	185.79 mmol g^{-1} h^{-1}	40.5 % at 420 nm	(Gopannagari, et al. 2017)
Ni-NG/CdS	300 W xenon lamp (> 420 nm)	1.0 M $(NH_4)_2SO_3$	263.5 mmol g^{-1} h^{-1}	48.2 % at 420 nm	(Zhao, et al., 2018)
Ca_1-NG/CdS	LED lamp (= 420 nm)	1.0 M $(NH_4)_2SO_3$	18.4 mmol g^{-1} h^{-1}	57.5 % at 420 nm	This work

Table S4. Ca concentration changes in 0.5 wt.% Ca_1-NG/CdS before and after 15 hours' photocatalytic H_2 evolution. **Related to Figure 4.**

	Before photocatalytic reaction	After photocatalytic reaction	Relative Change (%)
Ca concentration in 0.5 wt.% Ca_1-NG/CdS	0.0026 wt.%	0.0025 wt.%	3.84 %

Table S5. Non-radiative (τ_1), radiative (τ_2) and average (τ) lifetimes of time resolved photoluminescence spectra for CdS, 0.5 wt.% NG/CdS and 0.5 wt.% Ca_1-NG/CdS photocatalysts. **Related to Figure 5.**

Photocatalyst	τ_1 (ns)	τ_2 (ns)	τ (ns)
CdS	2.31	25.85	2.37
NG/CdS	1.71	21.51	1.88
Ca_1-NG/CdS	0.81	16.55	0.93